CHAPTER 4
RESULTS

4.1 Seaweeds collected and yields of methanolic extracts

A total of 14 species of seaweeds, consisting of seven Pheophyta, five Chlorophyta and two Rhodophyta were collected from Port Dickson for this study. The collected specimens include *Sargassum baccularia, Sargassum binderi, Sargassum siliquosom, Sargassum polycystum, Dictyota dichotoma, Turbinaria conoides, Padina australis, Chaetomorpha linum, Cladophora patentiramea*, *Caulerpa racemosa, Caulerpa lentillifera, Caulerpa* sp., *Gracilaria edulis* and *Gracilaria salicornia* (See Figures 4.1 – 4.3). Herbarium specimens of the seaweeds were made and deposited at the University of Malaya Seaweeds and Seagrasses Herbarium

(a) (b)

(c) (d)

Figure 4.1(a): The herbarium specimens of brown seaweeds
(a) *Sargassum baccularia* (c) *Sargassum siliquosom*
(b) *Sargassum binderi* (d) *Sargassum polycystum*

(e)

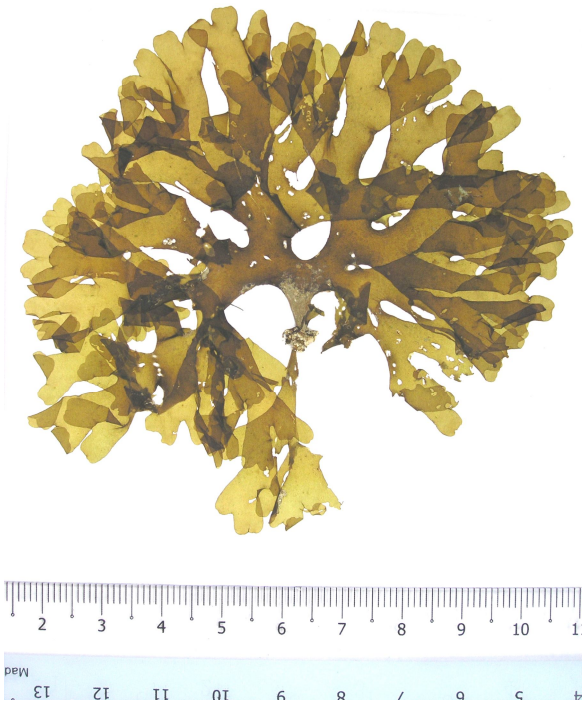

(f)

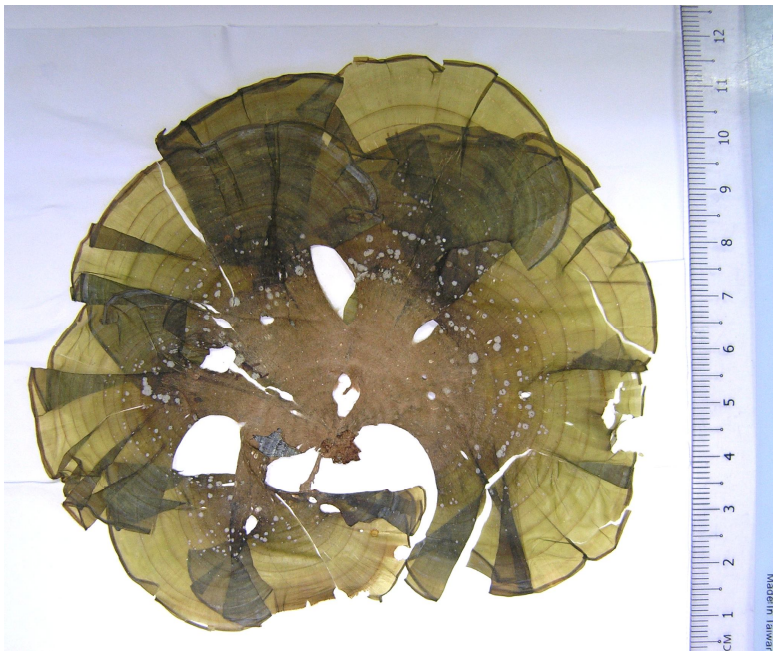

(g)

Figure 4.1(b): The herbarium specimens of brown seaweeds
(e) *Turbinaria conoides*
(f) *Dictyota dichotoma*
(g) *Padina australis*

(a)

(b)

Figure 4.2(a): The herbarium specimens of green seaweeds
a) *Chaetomorpha linum*
b) *Cladophora patentiramea*

(c)

(d)

(e)

Figure 4.2(b): The herbarium specimens of green seaweeds
(c) *Caulerpa lentilifera* (d) *Caulerpa racemosa* (e) *Caulerpa* sp

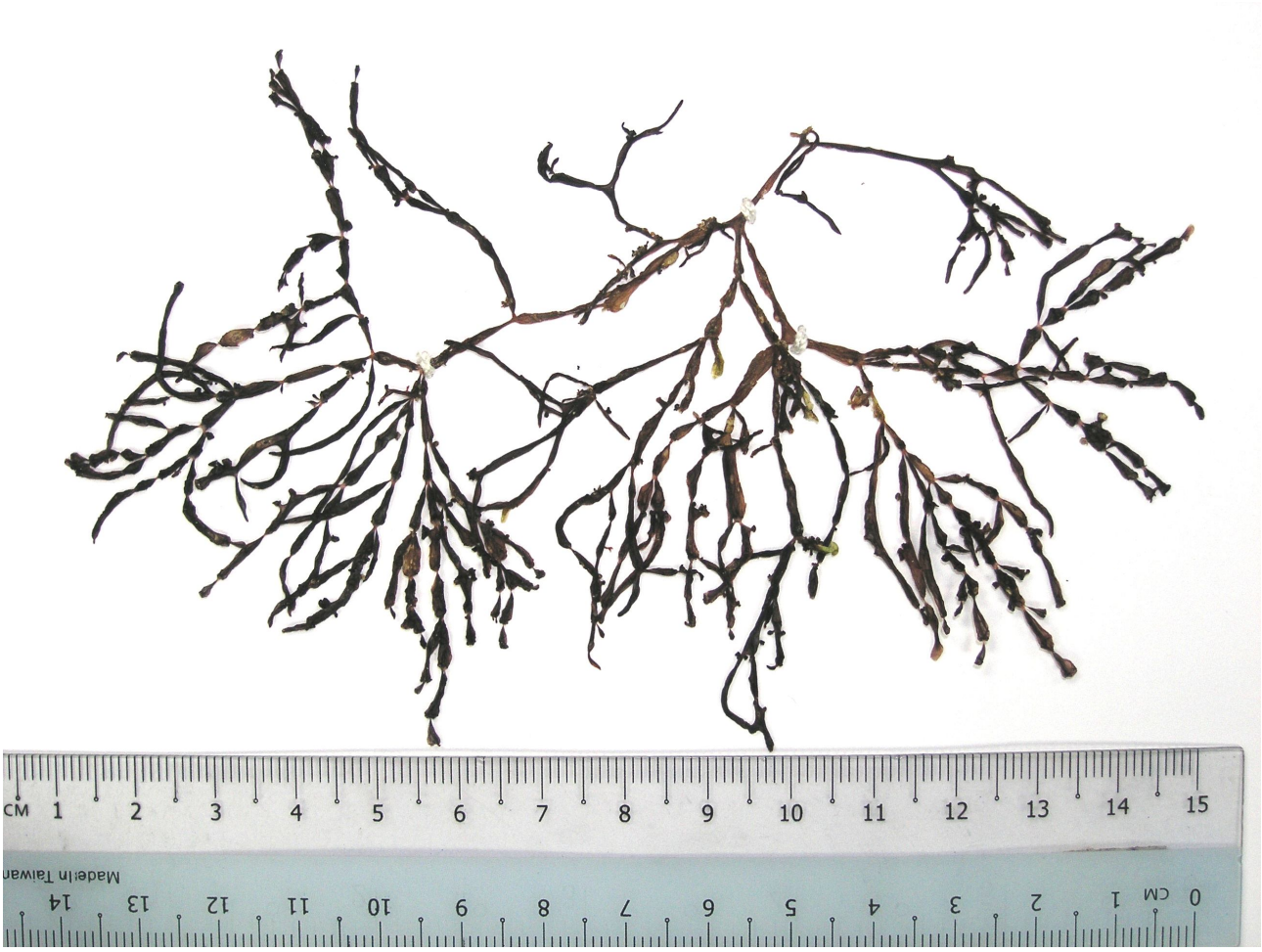

Figure 4.3: Herbarium of *Gracilaria salicornia* (red seaweed)

The yields of crude extracts prepared from the collected seaweeds are shown in Table 4.1. The yield of crude extracts varied among the seaweeds, ranging from 1.0-15.6% of their respective material dry weights. *Chaetomorpha linum* produced the highest methanolic extract yield followed by several brown seaweeds, including *Dictyota dichotoma, Padina austrialis* and *Saargassum baccularia.* Meanwhile, *Caulerpa racemosa* yielded the lowest amount of methanolic extract.

Table 4.1: Yields of crude extracts from 14 species of seaweeds collected from Port Dickson

Species	Dried material weight (g)	Yield of crude extract, g (% dry weight)
Brown seaweeds		
Sargassum baccularia	30.22	3.95 (13.1)
Sargassum binderi	10.03	0.44 (4.4)
Sargassum siliquosum	11.05	0.35 (3.2)
Sargassum polycystum	27.55	0.64 (2.3)
Dictyota dichotoma	8.07	1.21 (15.0)
Turbinaria conoides	30.06	2.86 (9.5)
Padina australis	24.97	3.67 (14.7)
Green seaweeds		
Chaetomorpha linum	4.24	0.66 (15.6)
Cladophora patentiramea	4.98	0.32 (6.4)
Caulerpa racemosa	93.70	0.91 (1.0)
Caulerpa lentillifera	11.16	0.37 (3.3)
Caulerpa sp.	13.08	1.42 (10.9)
Red seaweeds		
Gracilaria edulis	2.62	0.10 (3.8)
Gracilaria salicornia	30.47	2.12 (7.0)

4.2 Photo-cytotoxicity of methanolic extracts

Five of the 14 methanolic extracts showed > 50% HL60 cell-killing activity at 20 µg/mL after light irradiation. *Cladophora patentiramea* exhibited the highest photo-killing among the five extracts followed by *Gracilaria salicornia, Chaetomorpha linum and Turbinaria conoides.* In addition, *Dictyota dichotoma* demonstrated cytotoxic killing in both dark and light-irradiated conditions while *Sargassum polycystum* showed

marginal photo-cytotoxicity. Meanwhile, cytotoxicity and/or photo-cytotoxic activity were not observed among the remaining extracts, as showed in Figure 4.4.

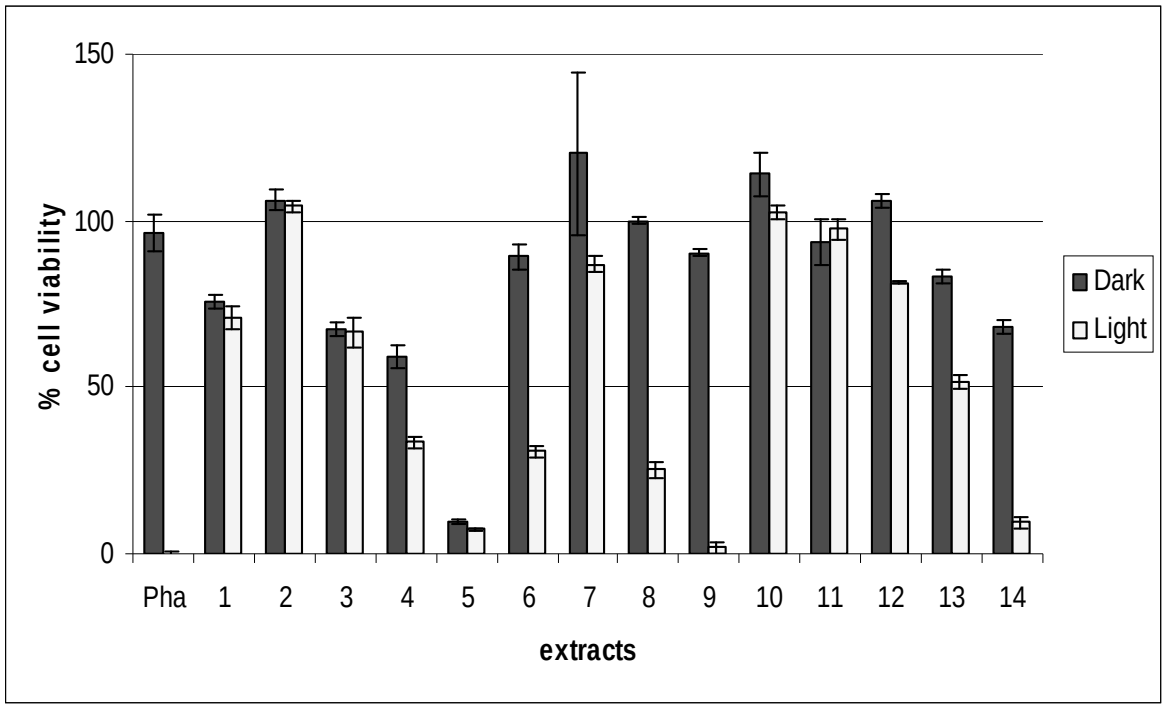

Figure 4.4: Viability of HL60 cells treated with 14 methanolic extracts at 20 μg/mL (dark-control and irradiated plates) with pheophorbide-*a* (Pha) as positive control

1- *Sargassum baccularia*
2- *Sargassum binderi*
3- *Sargassum siliquosum*
4- *Sargassum polycystum*
5- *Dictyota dichotoma*
6- *Turbinaria conoides*
7- *Padina australis*
8- *Chaetomorpha linum*
9- *Cladophora patentiramea*
10- *Caulerpa racemosa*
11- *Caulerpa lentillifera*
12- *Caulerpa sp.*
13- *Gracilaria edulis*
14- *Gracilaria salicornia*

Ideally, one of each seaweeds type was chosen for further investigation for potential photosensitisers in the study, namely *Turbinaria conoides* (brown), *Cladophora patentiramea* (green) and *Gracilaria salicornia* (red). However, the findings exclude the red seaweed species due the lack of raw materials for follow up.

4.3 Isolation of photo-cytotoxic compounds from *Turbinaria conoides* extract (Tur)

Approximately 1.5 kg of dried material was extracted with methanol to give about 33.87 g of methanolic extract. The fractionation and purification of the extract was carried out in a schematic flow as shown in Figure 4.5. The Tur extract was subjected to liquid-liquid partition with chloroform and yielded 5.41 g of chloroform fraction. Approximately 4.75 g extract was isolated via silica gel column chromatography to obtain 23 fractions. Subsequent purification was carried out on selected PDT-active fractions using HPLC to yield five compounds. Tur-10-4 (5.4 mg, green solid) was purified from Tur-10 (111.7 mg) using normal-phase HPLC at gradient of hexane and ethyl acetate while Tur-12-2 **(1)** (4.4 mg, dark green amorphous solid) and Tur-12-3 **(2)** (4.7 mg, dark green amorphous solid) were identified as the major peaks in Tur-12 using reversed-phase HPLC at gradient of acetonitrile and water. Tur-17-6 (2.8 mg, green solid) was also purified from Tur-17 using reversed-phase HPLC at gradient of acetonitrile and water. Tur-19 was isolated from the column chromatography of the extract and further purified to yield Tur-19-1 **(3)** (9.2 mg, black amorphous solid).

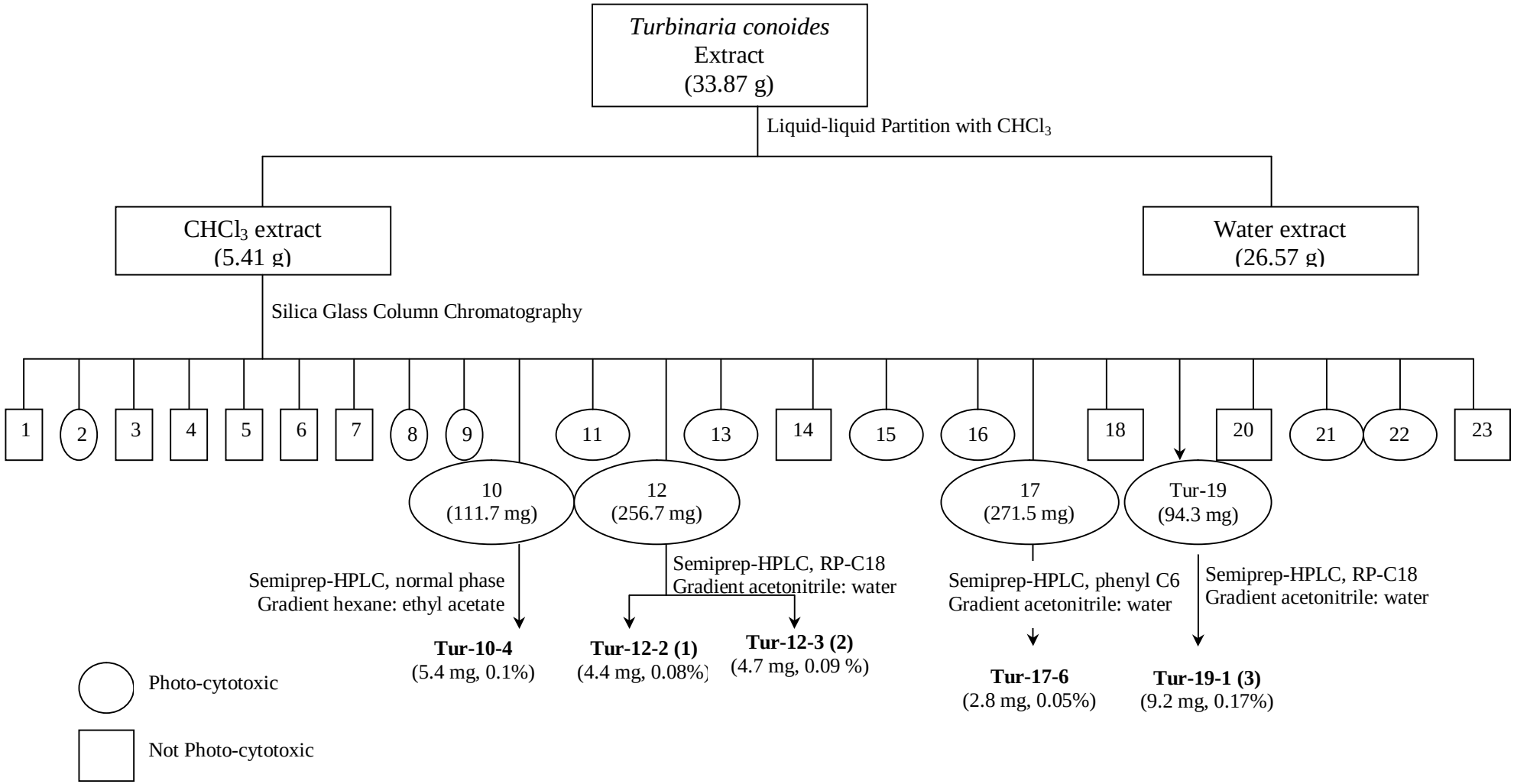

Figure 4.5: Isolation and purification process for *Turbinaria conoides* extract

4.3.1 Photo-cytotoxicity of fractions from partitioned chloroform extract of *Turbinaria conoides*

Twenty-three fractions separated by open column silica gel chromatography were collected as described previously. Thirteen of the fractions were active at 10 µg/mL with fraction 19, 21 and 22 demonstrated HL60 cell-killing activities only after light irradiation. Furthermore, fraction 2, 8-13 and 15-17 showed cytotoxicity in both dark and light-irradiated conditions (See Figure 4.6).

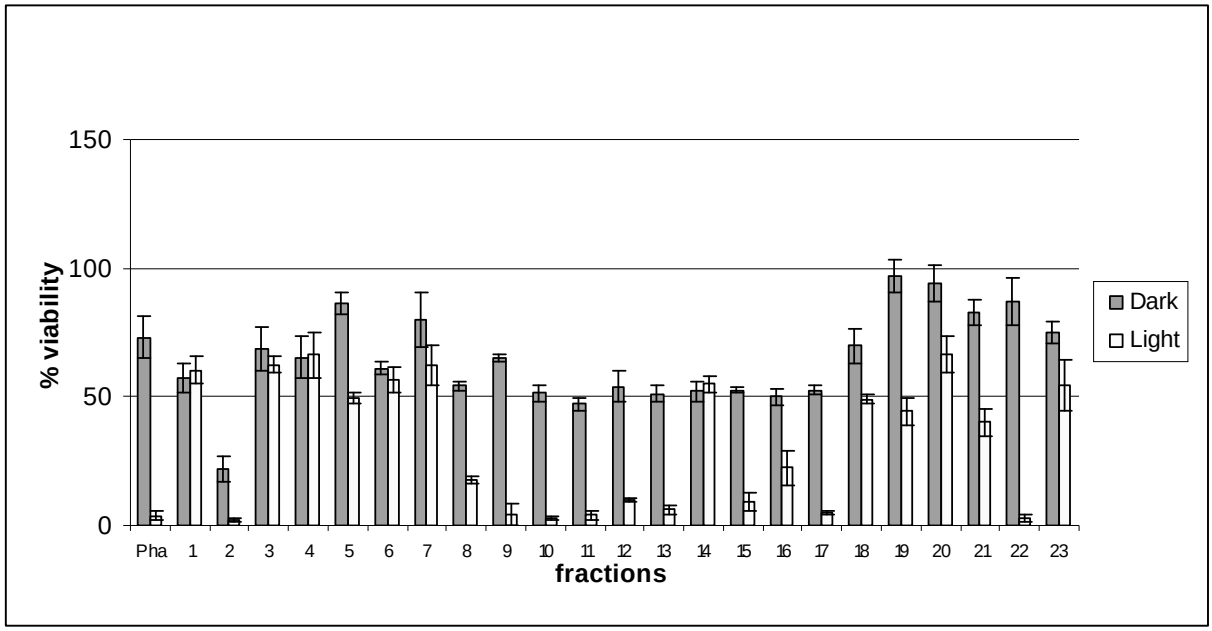

Figure 4.6: Viability of HL60 cells treated with 23 fractions collected from the first fractionation of *Turbinaria conoides* fxtract at 10 µg/mL

4.3.2 Identification of the active compounds from *Turbinaria conoides* extract

Three compounds were isolated and identified from *Turbinaria conoides (*Tur) extract, namely Tur-12-2, Tur-12-3 and Tur-19-1 in which were further identitified as pheophorbide-*a* methyl ester **(1)**, 13^2-hydroxypheophorbide-*a*- methyl ester **(2)** and pheophorbide-*a* **(3)**, respectively.

4.3.2.1 Identification of Tur-12-2

One of the active compounds isolated was Tur-12-2 (4.4 mg), which has UV-Vis profile as shown in Figure 4.7. The Soret max at 406 nm followed by a Q_y max of 662 nm indicates that Tur-12-2 has a chlorophyll-*a* type structure.

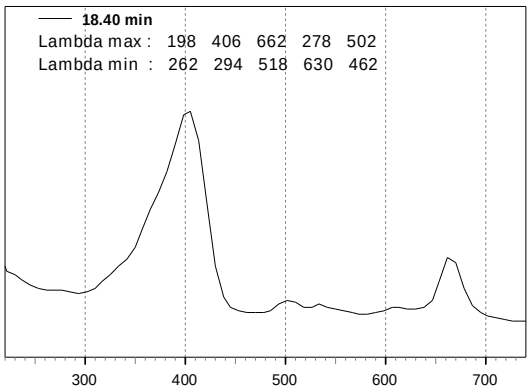

Figure 4.7: UV-Vis profile of Tur-12-2

The ^{1}H NMR spectrum of Tur-12-2 (Table 4.2) exhibited chemical shifts that were characteristic of typical chlorophyll-*a* type compounds. Three singlet methane signals observed at δ_H 9.56, 9.72 and 8.75 were respectively assigned as H-5, H-10 and H-20 of the cyclic tetrapyrrole core ring structure. The spectrum also exhibited a pair of vinylic proton signals at δ_H 7.91 (dd, J = 18, 11.5 Hz), 6.28 (d, J = 17.8 Hz) and 6.17 (d, J = 11.2), which were assigned as H-3^1 and H-3^2 and were shown to be correlated among themselves by the coupling constant values. These protons were found to resonate at a more deshielded region due to the presence of extended conjugation system in the tetrapyrrole ring.

In addition, the spectrum further depicted five methyl signals of typical chlorophyll-*a* type compound. Three of the signals were present as singlet at δ_H 3.36, 3.23 and 3.65 while a triplet and a doublet were observed respectively at δ_H 1.64 (J = 7.6 Hz) and δ_H 1.80 (J = 7.6 Hz). These signals were assigned to 2-CH_3, 7-CH_3, 12-CH_3, 8^2-CH_3 and 18-CH_3. Furthermore, another two singlet signals resonate at δ_H 3.82 and 3.52, were

identified as the methoxyl groups attached to C-13^2 and C-17^3 respectively. A few signals were also observed in the spectrum which belong to the methylene protons and methane protons, including δ_H 3.69 (J = 7.3 Hz), 2.49 (m), 2.27 (m), 6.26 (s), 4.51 (m) and 4.25 (m) that are assigned to 8^1-CH_2, 17^1-CH_2, 17^2-CH_2, 13^2-CH, 17-CH and 18-CH.

In comparison with the spectral data from the literature (Ling *et al.*, 2006), **(1)** was identified as pheophorbide-*a* methyl ester (Table 4.2) with the structure shown in Figure 4.8. The identity of Tur-12-2 was further confirmed by the mass data *m/z* 607.30 which corresponded to the molecular formula of $C_{36}H_{38}N_4O_5$.

Table 4.2: ^{1}H NMR chemical shifts of Tur-12-2 in $CDCl_3$

Position of H	Chemical shift, δ (ppm) in $CDCl_3$, J in Hz	
	Tur-12-2	pheophorbide-*a* methyl ester (Ling *et al.*, 2006)
18-CH_3	1.80 (d, J = 7.6)	1.73 (d, J = 7.3)
8^2-CH_3	1.64 (t, J = 7.6)	1.61 (t, J = 7.6)
17^2-CH_2	2.27 (m)	2.15-2.22 (m)
17^1-CH_2	2.49 (m)	2.44-2.49 (m)
7-CH_3	3.23 (s)	3.13 (s)
2-CH_3	3.36(s)	3.31 (s)
17^3-OCH_3	3.52 (s)	3.50 (s)
12-CH_3	3.65 (s)	3.68 (s)
8^1-CH_2	3.69(q, J = 7.3)	3.70 (q, J = 7.6)
13^2-CO_2CH_3	3.82 (s)	3.80 (s)
18-H	4.25 (m)	4.38 (q)
17-H	4.51 (m)	4.12 (br.d)
13^2-H	6.26 (s)	6.18 (s)
3^2-CH_2	6.28 (d, J = 17.8)	6.19(d)
	6.17 (d, J = 11.2)	6.09 (d)
3^1-H	7.91 (dd, J = 18,11.5)	7.89 (dd)
20-H	8.75 (s)	8.48 (s)
5-H	9.56 (s)	9.27 (s)
10-H	9.72 (s)	9.42 (s)
NH	not observed	-1.72

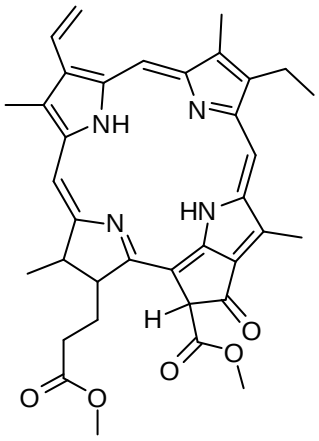

Figure 4.8: Pheophorbide-*a*- methyl ester **(1)**

4.3.2.2 Identification of Tur-12-3

The second active compound isolated from *Turbinaria conoides* was Tur-12-3 (4.7 mg). This compound showed characteristics of chlorophyll-*a* type derivative as indicted by the UV-Vis profile with Soret max of 406 nm and Q_y max of 662 nm (Figure 4.9).

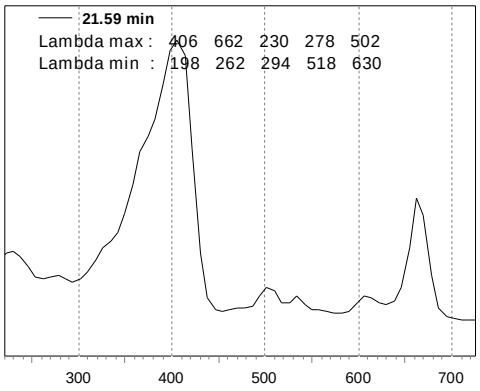

Figure 4.9: UV-Vis profile of Tur-12-3

The ^{1}H NMR spectrum of Tur-1-3 (Table 4.3) was found to be similar to pheophorbide-*a* methyl ester **(1)** which was of chlorophyll-*a* type compound. However, the singlet peak that was assigned to the proton attached to C-13^2 was not observed in the ^{1}H NMR spectrum of Tur-12-3 and a singlet peak at δ_H 5.42 that was assigned to a hydroxyl group was observed. This suggested that the proton could have been replaced by a hydroxyl group. The NMR values of Tur-12-3 also showed good agreement to the reported values of 13^2-hydroxypheophorbide-*a* ethyl ester (Chee *et al.*, 2005). However, a singlet signal was observed at δ_H 3.49 and the absence of a methylene proton

suggested the identity of Tur-12-3 to be 13^2-hydroxypheophorbide-*a*- methyl ester (See Figure 4.10).

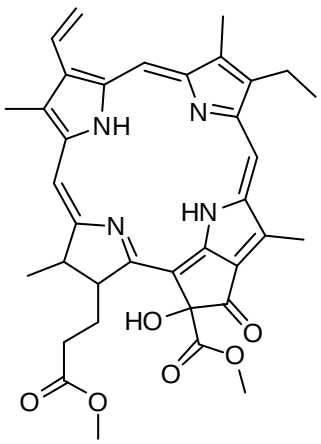

Figure 4.10: 13^2-hydroxypheophorbide-*a*- methyl ester **(2)**

Table 4.3: ^{1}H NMR chemical shift of Tur-12-3 in $CDCl_3$

Position of H	Chemical shift, δ (ppm) in $CDCl_3$, *J* in Hz	
	Tur-12-3	13^2 – hydroxypheophorbide ethyl ester (Chee *et al.*, 2005)
17^3-OCH_2CH_3	-	1.17 (t, *J* = 7)
18-CH_3	1.54 (d, *J* = 9)	1.71 (d, *J* = 7)
8^2-CH_3	1.63 (t, *J* = 9)	1.75 (d, *J* = 8)
17^2-CH_2	2.20 – 2.26 (m)	2.05 - 2.09 (m)
17^1-CH_2	2.44 – 2.53 (m)	2.26-2.31 (m)
7-CH_3	3.18 (s)	3.30 (s)
2-CH_3	3.35(s)	3.46 (s)
17^3-OCH_3	3.49 (s)	-
12-CH_3	3.55 (s)	3.64 (s)
8^1-CH_2	3.49 - 3.58 (br.q)	3.75 (q, *J* = 9)
13^2-CO_2CH_3	3.58 (s)	3.77 (s)
18-H	4.40-4.43 (q, *J* = 9)	4.52 (q, *J* = 7)
17-H	4.61 (d) (*J* = 9)	4.70 (br.d, *J* = 9)
13^2-OH	5.42 (s)	5.54 (s)
3^2-CH_2	6.23 (d, *J* = 18)	6.38(d, *J* =18)
	6.12 (d, *J* = 12)	6.23 (d, *J* = 12)
3^1-H	7.94 (dd, *J* = 18,12)	8.05 (dd, *J* = 18,12)
20-H	8.57 (s)	8.56 (s)
5-H	9.39 (s)	9.61 (s)
10-H	9.54 (s)	9.84 (s)
NH	-1.90	-1.65

4.3.2.3 Identification of Tur-19-1

The third compound isolated from *Turbinaria conoides* was Tur-19-1 (9.2 mg), which had UV-Vis profile of Soret max 410 nm followed by Q_y max of 662 nm, (Figure 4.11). In addition, MS analysis yielded *m/z* value of 593.3 (Figure 4.12). The structure was further verified using ^{1}H NMR (Table 4.4).

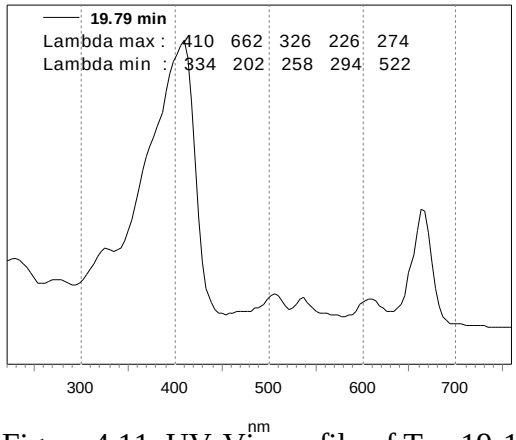

Figure 4.11: UV-Vis profile of Tur-19-1

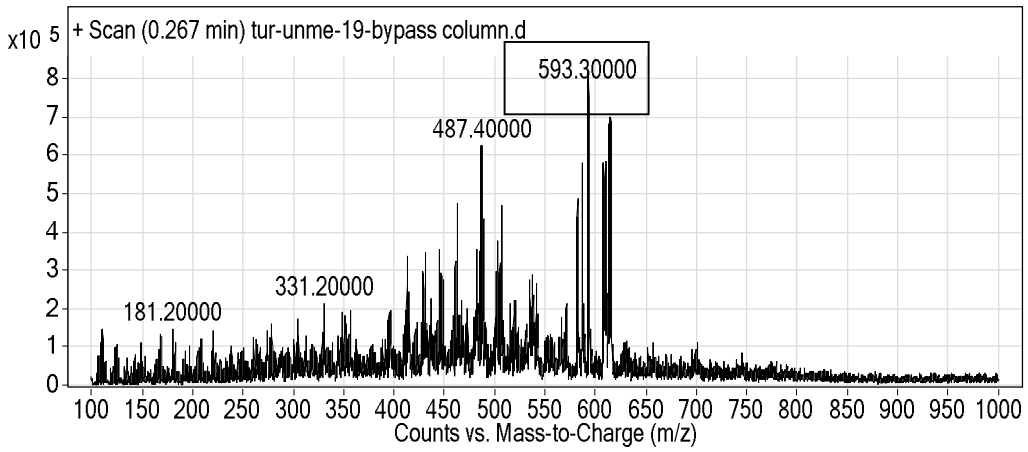

Figure 4.12: LC-MS data of Tur-19-1

The ^{1}H NMR spectrum of Tur-19-1 (Table 4.4) revealed that this compound was also similar to pheophorbide-*a*- methyl ester **(1)**. However, only one methoxyl group's chemical shift was observed in the spectrum, namely at δ_H 3.85 which was assigned as a methoxyl attached to C-13^2. Thus, by comparison with spectral data from the literature (Chee *et al.*, 2005), **(3)** was identified as pheophorbide-*a*.

Table 4.4: ^{1}H NMR chemical shifts of Tur-19-1 in $CDCl_3$

Position of H	Chemical shift, δ (ppm) in $CDCl_3$, *J* in Hz	
	Tur-19-1	pheophorbide-*a* (Chee *et al.*, 2005)
8-CH_3	1.79 (d, *J* = 8.1)	1.78 (d, *J* = 8)
8^2-CH_3	1.66 (t, *J* = 8.1)	1.66 (t, *J* = 8)
17^2-CH_2	2.28-2.33 (m)	2.33-2.38 (m)
17^1-CH_2	2.58-2.62 (m)	2.61-2.64 (m)
7-CH_3	3.23 (s)	3.19 (s)
2-CH_3	3.39 (s)	3.36 (s)
12-CH_3	3.69 (s)	3.57 (s)
8^1-CH_2	3.63-3.72 (m)	3.63 (q, *J* = 9)
13^2-CO_2CH_3	3.85 (s)	3.82 (s)
18-H	4.44-4.46 (m)	4.43 (q, *J* = 8)
17-H	4.19 (d, *J* = 8.1)	4.16 (br.d, *J* = 9)
13^2-H	6.31 (s)	6.31 (s)
3^2-CH_2	6.33 (d, *J* = 16.2)	6.29 (d, *J* = 18)
	6.15 (d, *J* = 10.8)	6.15 (d, *J* = 12)
3^1-H	7.93 (dd, *J* =18.9,10.8)	7.94 (dd, *J* =18,12)
20-H	8.56 (s)	8.54 (s)
5-H	9.38 (s)	9.32 (s)
10-H	9.51 (s)	9.42 (s)
NH	-1.71	-1.62

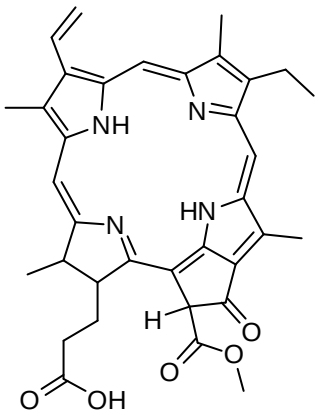

Figure 4.13: pheophorbide-*a* **(3)**

4.4 Isolation of photo-cytotoxic compounds from methylated extract of *Turbinaria conoides* (Tur-me)

Approximately 4.0 g of Tur methanolic extract was subjected to methylation to obtain 331.9 mg methylated extract. A semi-preparative HPLC collection with gradient of hexane and ethyl acetate at 12 ml/min shown in Table 4.5 obtained nine fractions which were active at 20 µg/mL. Tur-me-2 **(4)** (1.6 mg) was isolated as a pink solid from the semi-preparative collection while three other fractions were further purified using PTLC to obtain four compounds. Tur-me-4-2 **(1)** (2.3 mg, dark green amorphous solid) was isolated as a major component from Tur-4 using hexane: ethyl acetate 8:2 while Tur-me-6-3 **(2)** (0.7 mg, dark green solid) was isolated from Tur-6 with hexane: ethyl acetate 7:3. Tur-me-8-2 **(5)** (0.5 mg, dark green solid) and Tur-me-8-3 (0.5 mg, dark green solid) were purified from Tur-me-8 with hexane: ethyl acetate 6:4. The flow of isolation for Tur methylated extract is shown in Figure 4.14.

Table 4.5: Gradient system of hexane and ethyl acetate for semi-preparative normal-phase HPLC isolation of methylated *Turbinaria conoides* extract

Time (min)	% hexane	% ethyl acetate
0	90	10
10	90	10
30	30	70
40	0	100
80	0	100

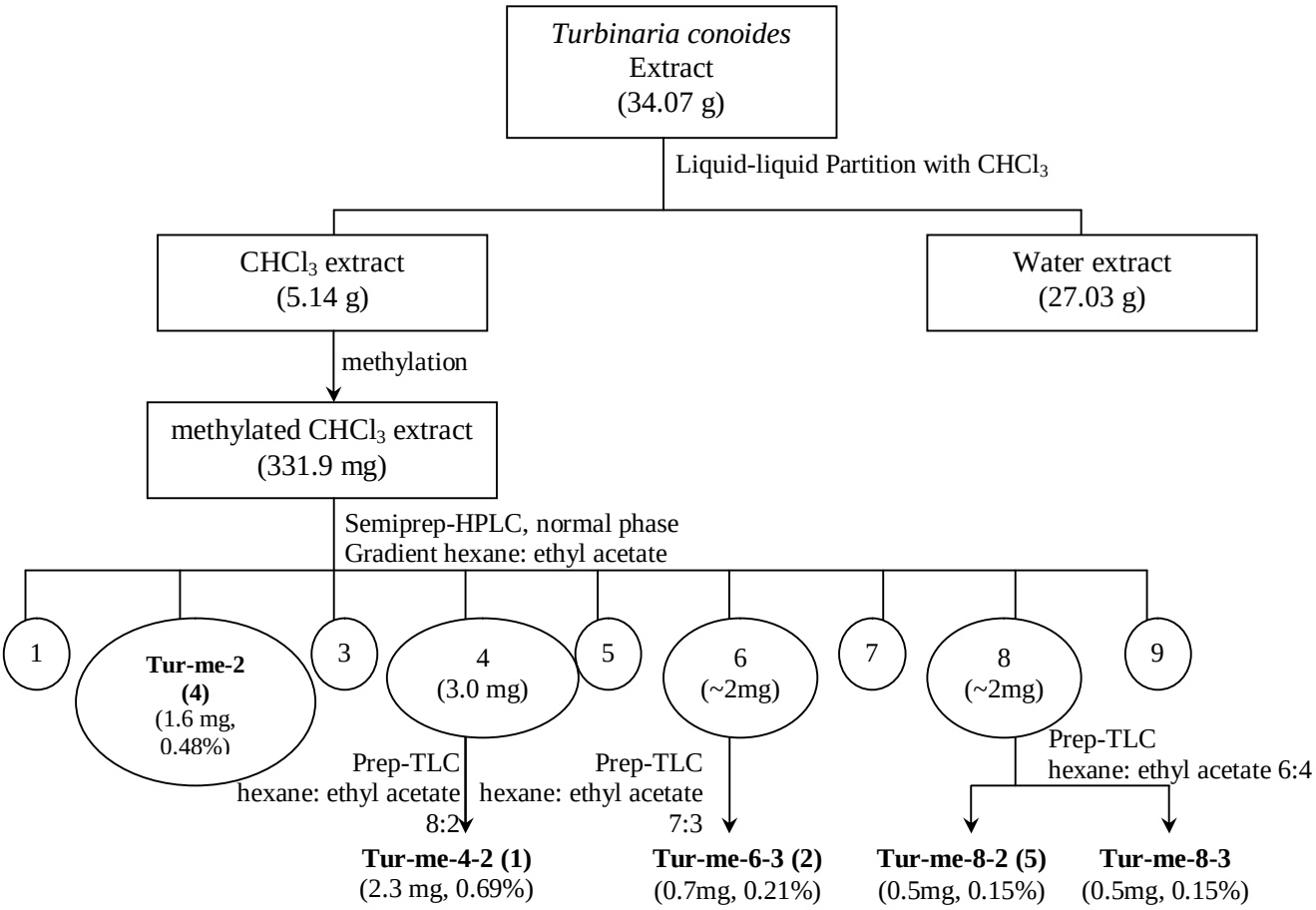

Figure 4.14: Isolation and purification process for methylated extract from *Turbinaria conoides*

4.4.1 Photo-cytotoxicity of fractions collected from methylated extract of *Turbinaria conoides*

Nine fractions were isolated from the methylated extract using HPLC method as described previously and were screened for photo-cytotoxicity at 10 µg/mL MTT (Figure 4.15). Fraction 9 showed significant photo-cytotoxicity while fractions 1 and 8 exhibited ~100% cell-killing in both dark and light-irradiated conditions. Fractions 2-7 also showed marginal cytotoxicity in the dark condition and strong cell-killing in light-irradiated condition.

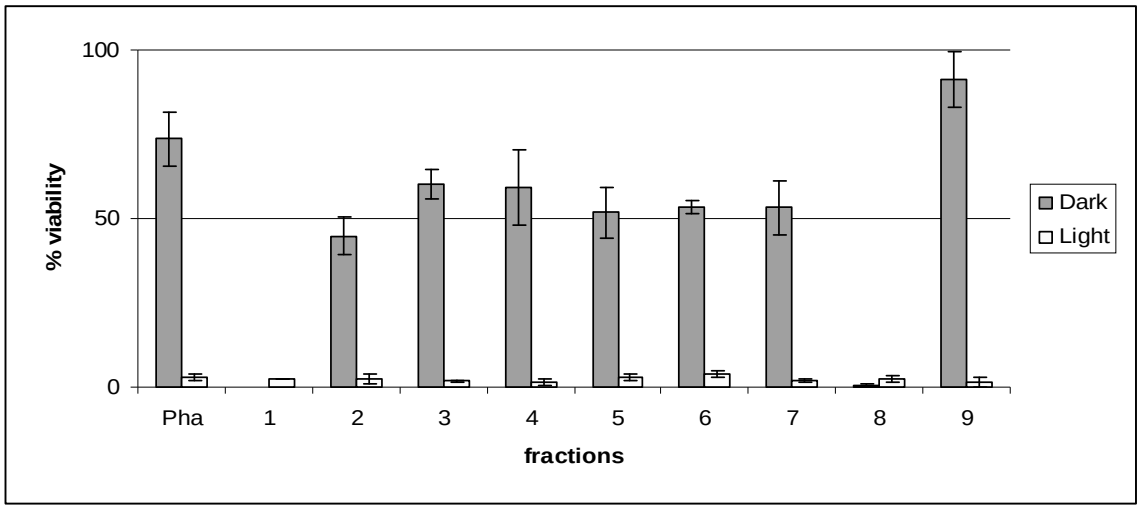

Figure 4.15: Viability of HL60 cells treated with nine fractions collected from the first fractionation of methylated extract of *Turbinaria conoides*. The fractions were tested at 10 µg/mL

4.4.2 Identification of active compounds from methylated extract of *Turbinaria conoides*

A total of four compounds were isolated from methylated extract of *Turbinaria conoides* (Tur-me) including Tur-me-2, Tur-me-4-2, Tur-me-6-3 and Tur-me-8-2 in which subsequently characterized to be purpurin-18 methyl ester **(4),** pheophorbide-*a* methyl ester **(1)**, 13^2-hydroxypheophorbide-*a* methyl ester **(2)** and 13^2-methoxyl-pheophorbide-*a* methyl ester **(5).**

4.4.2.1 Identification of Tur-me-2

The first compound Tur-me-2 (1.6 mg) exhibited UV-vis profile that is unique to a purpurin derivative (Naylor and Keely, 1998), with a Soret max of 406 nm and Q_y max of 694 nm (See Figure 4.16).

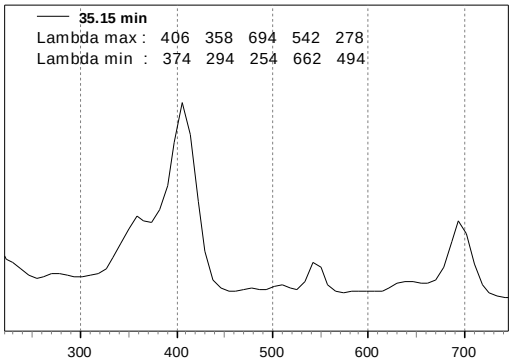

Figure 4.16: UV-Vis profile of Tur-me-2

Purpurin-18 is a chlorin-based structure with a six-membered anhydride ring due to the oxidative cleavage of the isopentanone ring E (Brandis *et al.*, 2006). It has strong absorption at 698 nm (Nyman and Hynninen, 2004) or 700 nm (Brandis *et al.*, 2006) with the calculated mass of 564.63.

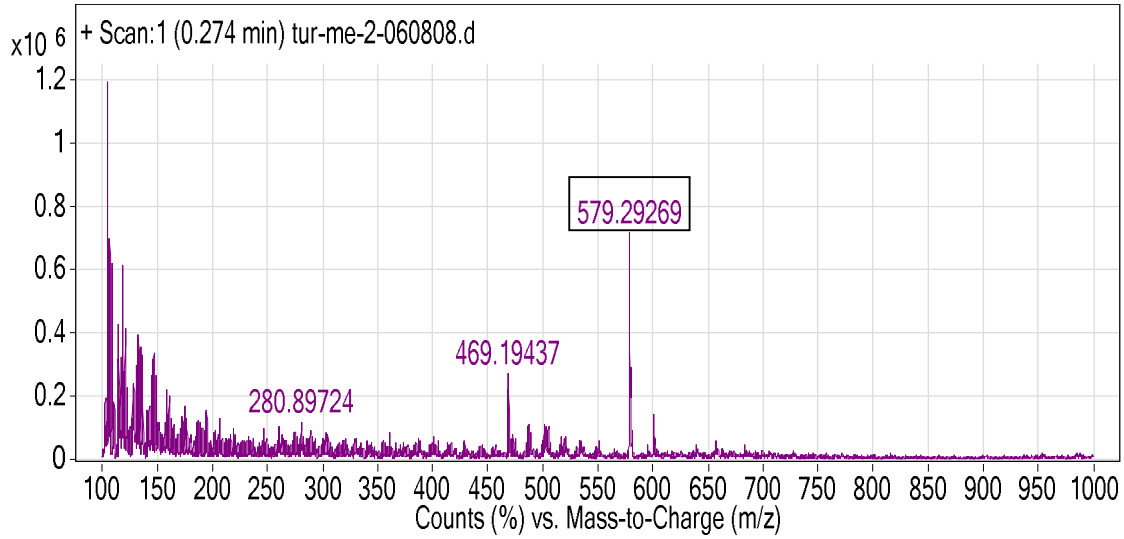

Figure 4.17: LC-MS data of Tur-me-2

MS analysis of Tur-me-2 gave the *m/z* value of 579.3 (Figure 4.17), an extra mass value of 15 units as compared to that of purpurin-18, which was equivalent of a methyl group. Thus, a methyl ester form of purpurin-18 was proposed. A comparison of the UV-Vis data was made with a similar compound that has been isolated from sedimentary organic matter (Ocampo and Repeta, 1999) in the following table (See Table 4.6).

Table 4.6: Comparison of UV-Vis absorbance and *m/z* values between Tur-me-2 and purpurin-18 methyl ester

	Tur-me-2	Purpurin-18 methyl ester (Ocampo and Repeta, 1999)
UV-Vis abs (nm)	358, 406, 542, 694 (dissolved in HPLC eluted solvent)	410, 546, 592, 698 (dissolved in acetone)
m/z values	579 [$M+H^+$]	578 [M^+]

As the data obtained is similar to that of the literature, Tur-me-2 is proposed to be purpurin-18 methyl ester (Figure 4.18). Nevertheless, NMR spectroscopy is required for further validation of Tur-me-2.

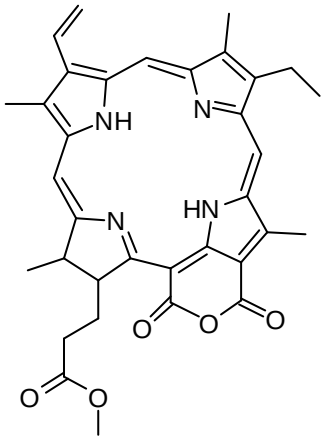

Figure 4.18: Purpurin-18 methyl ester **(4)**

4.4.2.2 Identification of Tur-me-4-2

Tur-me-4-2 (2.3 mg) depicted a UV-Vis profile of chlorophyll-*a* type derivative with Soret max of 406 nm and Q_y max of 662 nm (See Figure 4.19).

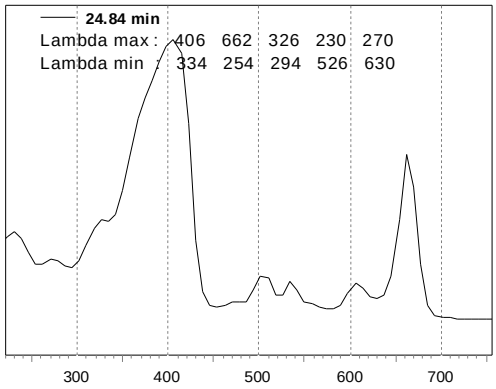

Figure 4.19: UV-Vis profile of Tur-me-4-2

Tur-me-4-2 was eluted at the same retention time as Me-Pha in-house standard via HPLC co-injection method (R_t = 24.82 minutes). Subsequent MS characterisation confirmed the identity of Tur-me-4-2 as pheophorbide-*a* methyl ester **(1)** with *m/z* value of 607.2923, as described in Figure 4.20.

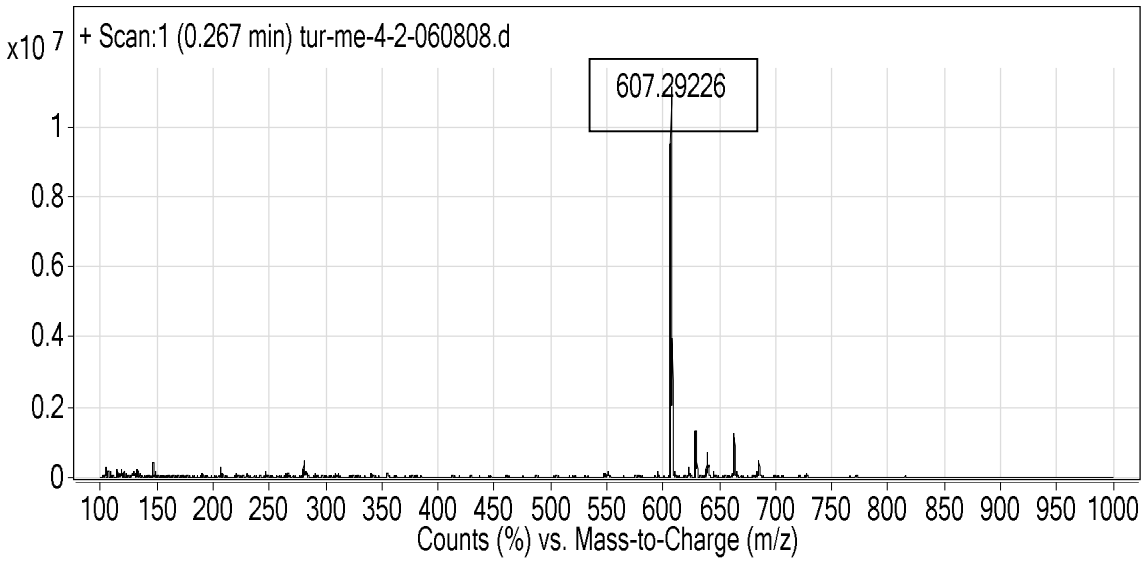

Figure 4.20: LC-MS data of Tur-me-4-2

4.4.2.3 Identification of Tur-me-6-3

Tur-me-6-3 (0.7 mg) displayed UV-Vis profile of chlorophyll-*a* type (Soret max 406 nm and Q_y max 664 nm) (See Figure 4.21) and eluted at the same retention time with OH-Pha **(2)** in-house standard via RP-HPLC co-injection method (R_t = 22.31 minutes).

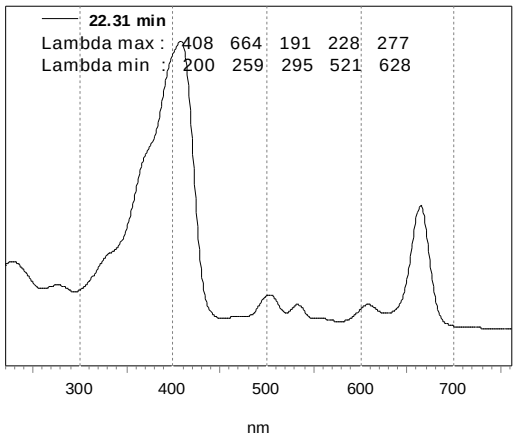

Figure 4.21: UV-Vis profile of Tur-me-6-3

Further validation via MS and obtained *m/z* value of 623.1 (See Figure 4.22) thus proved the identity of Tur-me-6-3 as 13^2-hydroxypheophorbide-*a* methyl ester **(2)** (See Figure 4.10).

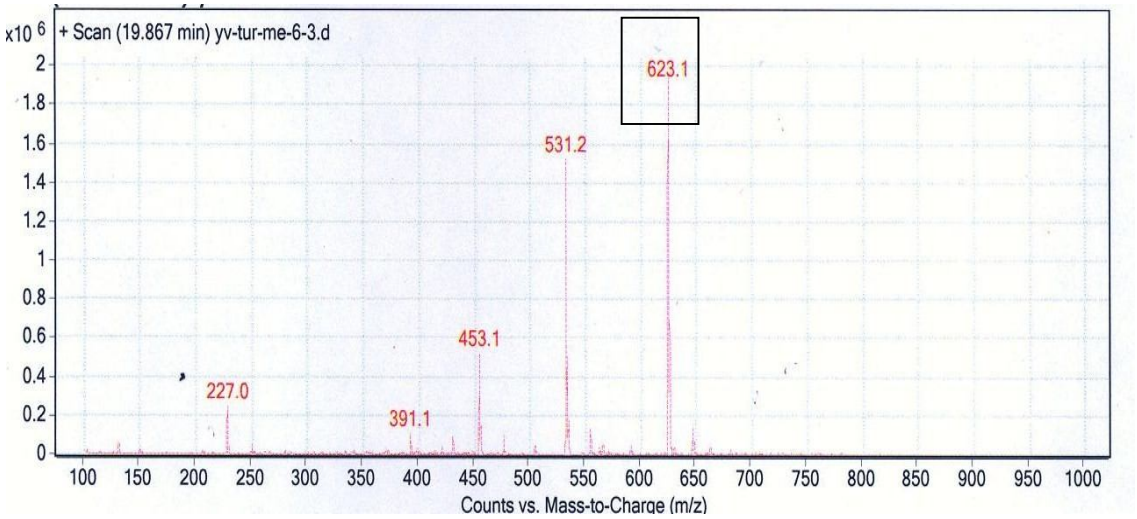

Figure 4.22 LC-MS data of Tur-me-6-3

4.4.2.4 Identification of Tur-me-8-2

Tur-me-8-2 (0.5 mg) also exhibited a typical UV-Vis profile of that of chlorophyll-*a* derivative (See Figure 4.23) and was further characterised with MS, which gave an *m/z* value of 637.2918 (See Figure 4.24).

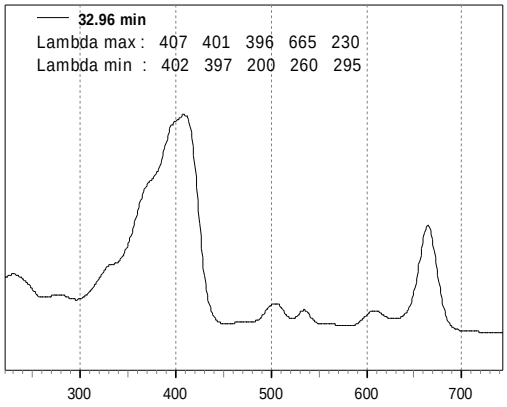

Figure 4.23: UV-Vis profile of Tur-me-8-2

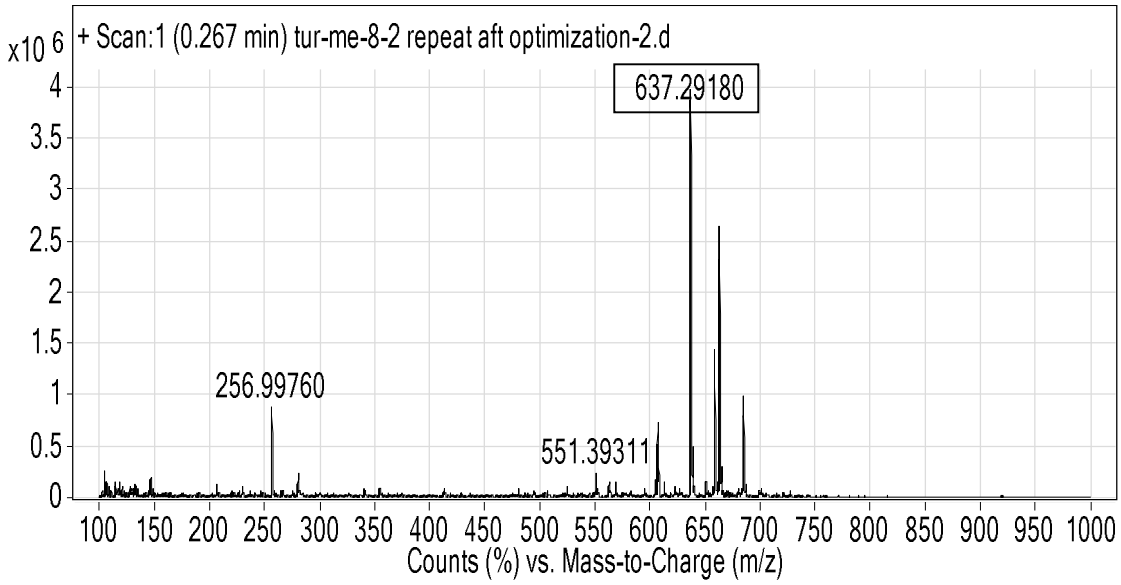

Figure 4.24: LC-MS data of Tur-me-8-2

^{1}H-NMR analysis of Tur-me-8-2 (See Table 4.7) again showed the characteristics of chlorophyll-*a* type compound. A singlet peak at δ_H 3.34 was assigned to a methoxyl group attached at C-17^3. This was reasonable as the methylation probably resulted in the esterification of the free acid at the C17^3 position to its methyl ester form. Furthermore, the presence of another singlet peak at δ_H 3.42 was assigned to a methoxyl group that was deduced to have replaced the hydroxyl group at C-13^2 due to the absence of singlet signal at δ_H 5.54. The NMR data was compared with the reported literature values of 13^2-hydroxypheophorbide ethyl ester (Chee *et al.*, 2005) to distinguish the difference in

the observed chemical shifts. Combining all these data, the compound was proposed to be a 13^2-methoxyl-pheophorbide-*a* methyl ester **(5)** (Figure 4.25). In addition, the proposed structure's calculated mass has also matched the *m/z* value obtained from MS.

Table 4.7: ^{1}H NMR chemical shift of Tur-me-8-2 in $CDCl_3$

Position of H	Chemical shift, δ (ppm) in $CDCl_3$, *J* in Hz	
	Tur-me-8-2	13^2–hydroxypheophorbide ethyl ester (Chee *et al.*, 2005)
17^3-OCH_2CH_3	-	1.17 (t, *J* = 7)
18-CH_3	1.58 (d, *J* = 7.5)	1.71 (d, *J* = 7)
8^2-CH_3	1.63 (t, *J* = 10)	1.75 (d, *J* = 8)
17^2-CH_2	1.92 – 2.01 (m)	2.05-2.09 (m)
17^1-CH_2	2.25 – 2.28 (m)	2.26-2.31 (m)
7-CH_3	3.19 (s)	3.30 (s)
2-CH_3	3.24(s)	3.46 (s)
17^3-OCH_3	3.34 (s)	-
13^2-OCH_3	3.42 (s)	-
12-CH_3	3.59 (s)	3.64 (s)
8^1-CH_2	3.61 (br.q, *J* = 10)	3.75 (q, *J* = 9)
13^2-CO_2CH_3	3.75 (s)	3.77 (s)
18-H	4.47 (m)	4.52 (q, *J* = 7)
17-H	not observed	4.70 (br.d, *J* = 9)
13^2-OH	-	5.54 (s)
3^2-CH_2	6.33 (d, *J* = 15)	6.38_a (d, *J* = 18)
	6.22 (d,*J* = 10)	6.23_b(d, *J* = 12)
3^1-H	7.97 (m)	8.05 (dd, *J* = 18,12)
20-H	8.54 (s)	8.56 (s)
5-H	9.39 (s)	9.61 (s)
10-H	9.53 (s)	9.84 (s)
NH	-1.71	-1.65

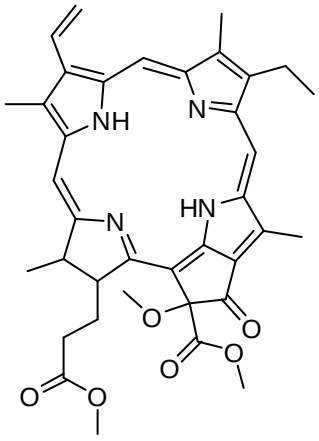

Figure 4.25: 13^2-methoxyl- pheophorbide-*a* methyl ester **(5)**

4.5 Isolation of photo-cytotoxic compounds from the extract of *Cladophora patentiramea*

Approximately 1.6 kg of dried material was extracted and partitioned with chloroform to obtain 5.6 g of chloroform extract. It was subjected to semi-preparative normal-phase HPLC isolation at gradients of hexane: ethyl acetate (Table 4.8) to yield four fractions that were active at 10 µg/mL. Further purification of cla-7 using semi-preparative reversed-phase HPLC with a gradient of acetonitrile and water yielded cla-7-3 (3.1 mg, yellow solid). Meanwhile, inactive fractions with major yields, namely fractions 1, 2 and 4 were subjected to methylation. All treated fractions were found to be active at 20 µg/mL and therefore were further investigated. Further purification of the fractions with reversed-phase HPLC using acetonitrile and water yielded cla-me-1 **(6)** (3.4 mg, green-black amorphous solid), cla-me-2-1 **(2)** (4.0 mg, dark green amorphous solid), cla-me-2-2 **(1)** (5.9 mg, dark green amorphous solid), cla-me-4-2 **(7)** (5.3 mg, yellow-brownish solid), cla-me-4-3 **(8)** (5.2 mg, yellow-brownish solid) and cla-me-4-5-4 **(9)** (4.8 mg, green solid). The protocols for the isolation of the photo-active compounds from Cla extract is shown in Figure 4.26.

Table 4.8: Gradient system of hexane and ethyl acetate for semi-preparative normal-phase HPLC isolation of *Cladophora patentiramea* extract

Time (min)	% hexane	% ethyl acetate
0	95	5
10	95	5
60	55	45
70	0	100
90	0	100

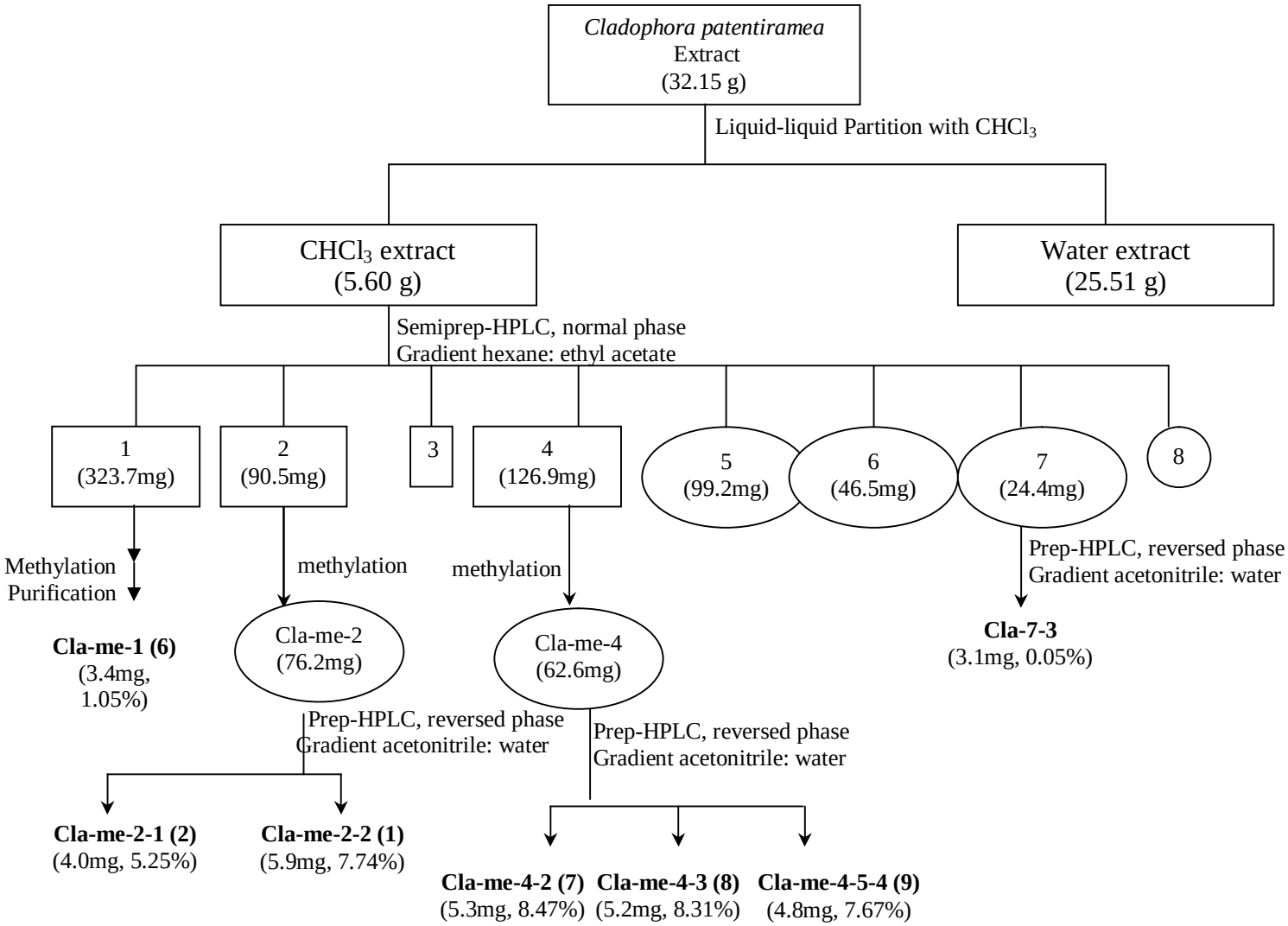

Figure 4.26 : Isolation and purification process for *Cladophora patentiramea* extract

4.5.1 Photo-cytotoxicity of fractions from the extract of *Cladophora patentiramea*

Eight fractions collected from HPLC fractionation showed variable photo-cytotoxicity only at 20 µg/mL in the MTT screening assay (See Figure 4.27). The more polar fractions, namely fractions 5-8, exhibited significant photo-cytotoxicity as compared to the less polar fractions (fraction 1-4).

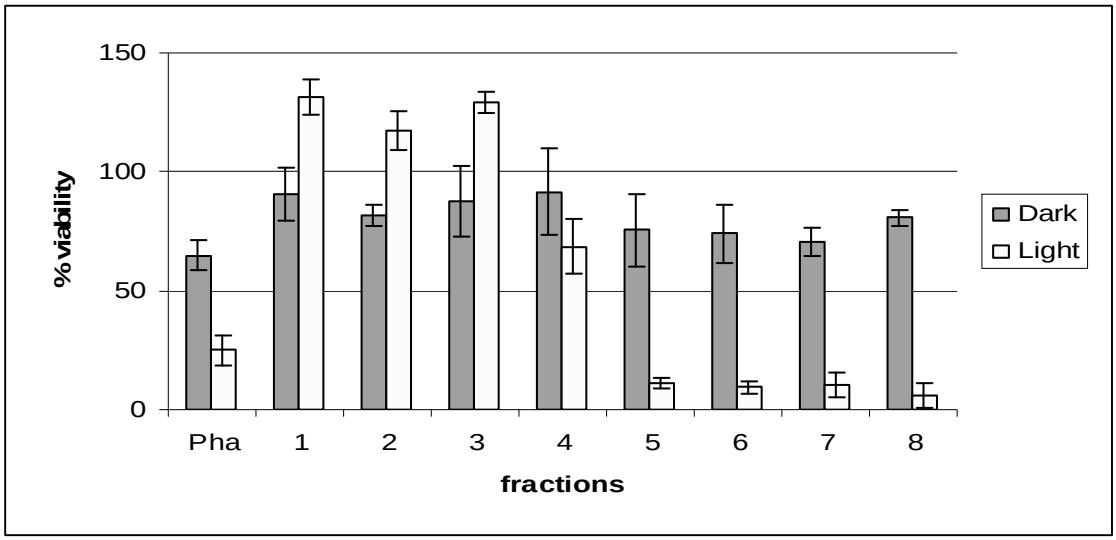

Figure 4.27: Viability of HL60 cells treated with eight fractions of the eExtract from *Cladophora parentiramea* . The fractions were tested at 20 µg/mL

However, the subsequent methylated products from fractions 1, 2 and 4 were found to show photo-cytotoxicity at 20 µg/mL as compared to their respective unmethylated fractions, as shown in Figure 4.28.

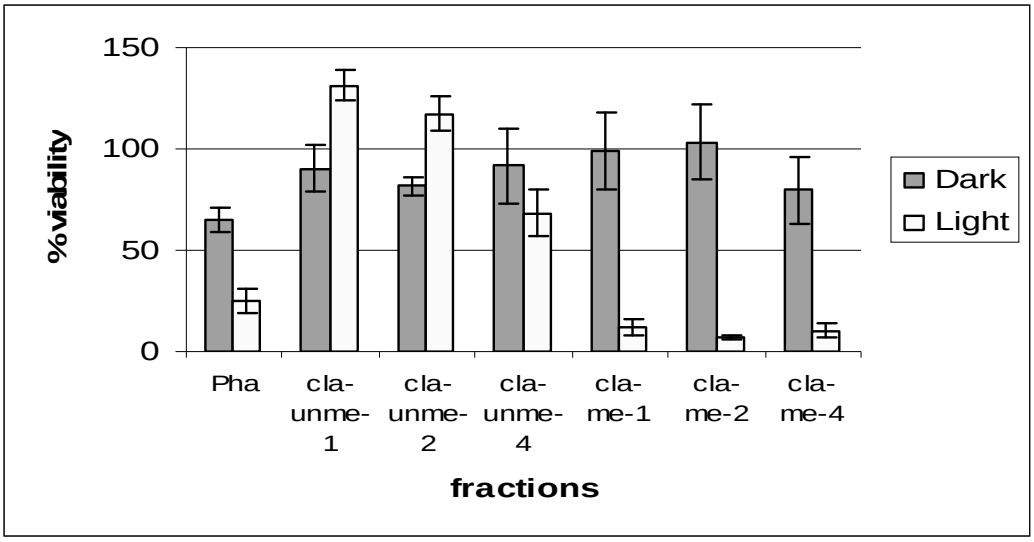

Figure 4.28: Comparison of HL60 cells viability for fraction 1, 2 and 4 before and after methylation at 20 µg/mL

4.5.2 Identification of active principles from *Cladophora patentiramea*

4.5.2.1 Identification of Cla-me-1

Cla-me-1 (3.4 mg) showed UV-Vis profile with Soret max of 398 nm and Q_y max of 670 nm (See Figure 4.29), which is of chlorophyll-*a* type. The compound was subjected to further characterization by MS (See Figure 4.30) and NMR (See Table 4.9)

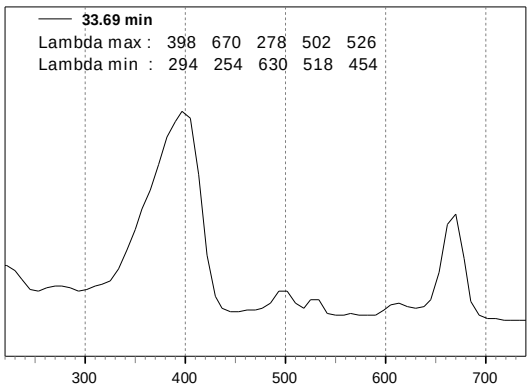

Figure 4.29: UV-Vis profile of Cla-me-1

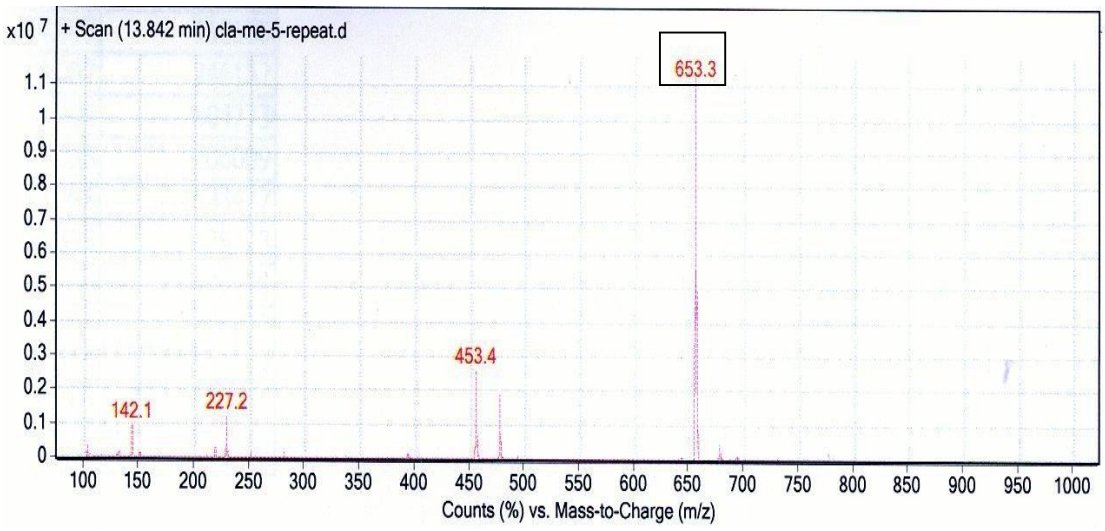

Figure 4.30: LC-MS data of Cla-me-1

The high *m/z* value obtained, namely 653.3 suggested the presence of a six-membered ring E in the structure proposed for Cla-me-1. The data matched very closely with the reported values of 15^1-hydroxypurpurin-7-lactone ethyl methyl diester (Chee *et al.*, 2005). However, a singlet resonance at δ_H 5.60 assigned to a hydroxyl group was not observed in the experimental data (See Table 4.9). In addition, a singlet signal that was assigned to a methoxyl group was observed, therefore suggesting that the replacement of hydroxyl group at C-15^1 with the methoxyl group. The absence of a triplet signal of 17^3-OCH_2CH_3 in the NMR spectral data suggested that Cla-me-1 is the methyl ester form of the reported compound. Consequently, the proposed structure's calculated mass also matched with the mass values obtained.

Table 4.9: ^{1}H NMR chemical shift of Cla-me-1 in $CDCl_3$

Position of H	Chemical shift, δ (ppm) in $CDCl_3$; *J* in Hz	
	Cla-me-1	15^1-methoxypurpurin-7-lactone methyl diester (Chee *et al.*, 2005)
17^3-OCH_2CH_3	-	1.10 (t, *J* = 7)
8^2-CH_3	1.59 (t)	1.75 (t)
18-CH_3	1.51(d)	1.65 (d)
17^2-CH_2	2.27 – 2.35 (m)	2.44 – 2.50 (m)
17^1-CH_2	2.53 – 2.61 (m)	2.58 – 2.64 (m)
7-CH_3	3.37 (s)	3.32 (s)
2-CH_3	3.46 (s)	3.48 (s)
17^3-OCH_3	3.49 (s)	-
12-CH_3	3.53(s)	3.79 (s)
15^1-OCH_3	3.60 (s)	-
15^1-OH	-	5.60 (s)
15^1-CO_2CH_3	3.84 (s)	3.94 (s)
8^1-CH_2	3.69(br. d, *J* = 10)	3.82 (br. d, *J* = 9)
17-H	4.60 (q, *J* = 9)	4.12 (br.d, *J* = 9)
18-H	4.37 (br.d, *J* = 7)	4.50 (q, *J* = 7)
3^2-CH_2	6.11(d, *J* = 18)	6.38 (d, *J* = 18)
	6.28 (d, *J* = 12)	6.23 (d, *J* = 12)
3^1-H	7.95 (dd, *J* = 18,12)	8.05 (dd, *J* = 18,12)
20-H	8.64 (s)	8.56 (s)
5-H	9.46 (s)	9.61 (s)
10-H	9.69 (s)	9.84 (s)
NH	-1.12	-1.02

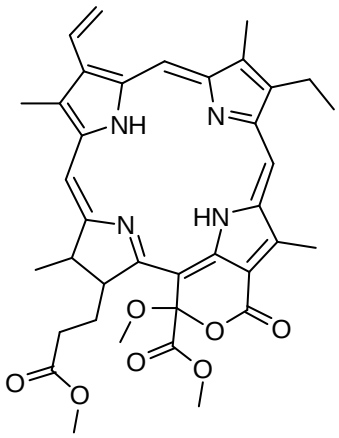

Figure 4.31: 15^1-methoxypurpurin-7-lactone methyl diester **(6)**

4.5.2.2 Identification of Cla-me-2-1

Cla-me-2-1 (4.0 mg) was isolated and eluted at the same retention time as that of OH-Pha **(2)** in house standard via RP-HPLC co-injection (R_t = 22.46 minutes). The MS

analysis gave an *m/z* value of 623.3, confirming the identity of cla-me-2-1 to be **(2)** (See Figure 4.10).

4.5.2.3 Identification of Cla-me-2-2

Cla-me-2-2 (5.9 mg) was isolated and eluted at the same retention time as that of the in house standard Me-Pha **(1)** (R_t = 24.30 minutes) co-injected in the HPLC analysis. MS analysis yielded an *m/z* value of 607.3 and identified Cla-me-2-2 as pheophorbide-*a* methyl ester **(1)** (See Figure 4.8).

4.5.2.4 Identification of Cla-me-4-2

Cla-me-4-2 (5.3 mg) was characterized as a chlorophyll-*b* type compound based on its UV-Vis profile at Soret max of 438 nm and Q_y max of 654 nm (Figure 4.32). It was also observed that its retention time on RP-HPLC run was shorter than that of other chlorophyll-*a* derivatives (approximately 18 minutes) indicating that chlorophyll-*b* derivatives are more polar than chlorophyll-*a* derivatives. MS analysis on cla-me-4-2 gave an *m/z* value of 637.3. This compound was further characterised by ^{1}H-NMR and the data are shown in Table 4.10.

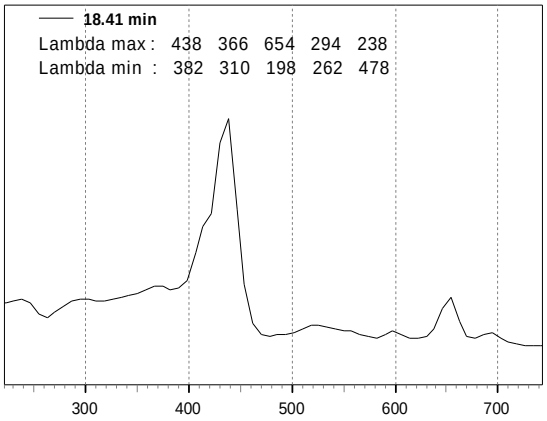

Figure 4.32: UV-Vis profile of Cla-me-4-2

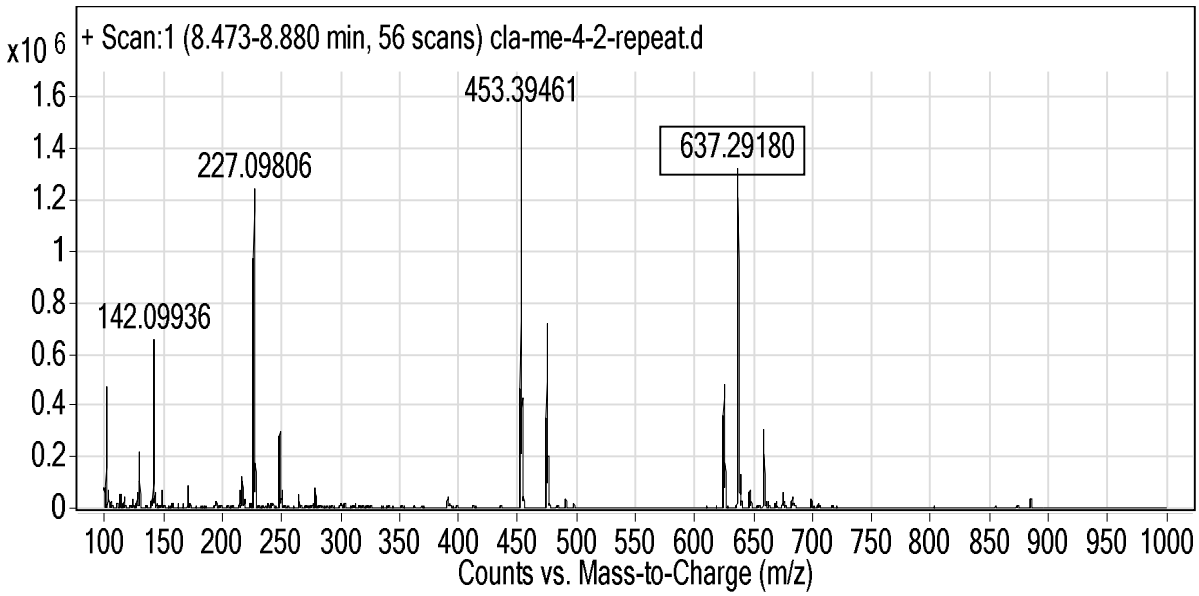

Figure 4.33: LC-MS data of Cla-me-4-2

The NMR data of Cla-me-4-2 (See Table 4.10) was comparable to that of 13^2-hydroxypheophorbide-*b* ethyl ester reported in the literature (Chee *et al.*, 2005). The presence of a singlet peak at δ_H 11.15 that was assigned to an aldehyde group identified Cla-me-4-2 as a chlorophyll-*b* derivative. Another singlet peak at δ_H 5.25 assigned to a hydroxyl group was likely to be attached at C-13^2 position. It was also noted that the chemical shift of hydrogen groups at C5 was higher than at C-10, as compared to the NMR values of chlorophyll-*a* type photosensitisers. This is probably due to the presence of a carbonyl group at C-7 which caused electron transfer in the cyclic tetrapyrrole and this could induce a deshielding effect other proton at C-5.

Table 4.10: ^{1}H NMR chemical shifts of Cla-me-4-2 in $CDCl_3$

Position of H	Chemical shift, δ (ppm) in $CDCl_3$, *J* in Hz	
	Cla-me-4-2	13^2-Hydroxypheophorbide-*b* ethyl ester (Chee *et al.*, 2005)
17^3-OCH_2CH_3	-	1.19 (t, *J* = 7)
8^2-CH_3	1.80 (t, *J* = 8)	1.86 (t, *J* = 8)
18-CH_3	1.62 (d, *J* = 7)	1.73 (d, *J* = 7)
17^2-CH_2	2.28 (t)	2.09 – 2.13 (m)
17^1-CH_2	2.31-2.41 (m)	2.56 – 2.63 (m)
2-CH_3	3.33 (s)	3.43 (s)
17^3-OCH_3	3.51 (s)	-
12-CH_3	3.59 (s)	3.66 (s)
8^1-CH_2	3.68 (m)	3.73 (q, *J* = 9)
13^2-CO_2CH_3	3.66 (s)	3.76 (s)
17-H	4.59 (br.d, *J* = 8)	4.70 (br.d, *J* = 9)
18-H	4.40 (q, *J* = 7)	4.51 (q, *J* = 7)
13^2-OH	5.25 (s)	5.58 (s)
3^2-CH_2	6.33 (d, *J* = 18)	6.41 (d, *J* = 18)
	6.18 (d, *J* = 12)	6.26 (d, *J* = 12)
3^1-H	7.92 (dd, *J*=18, 12)	8.04 (dd, *J*=18,12)
20-H	8.52 (s)	8.64 (s)
5-H	10.71 (s)	10.47 (s)
10-H	9.71 (s)	9.74 (s)
7^1-CHO	11.15 (s)	11.17 (s)
NH	- 1.60	- 1.62

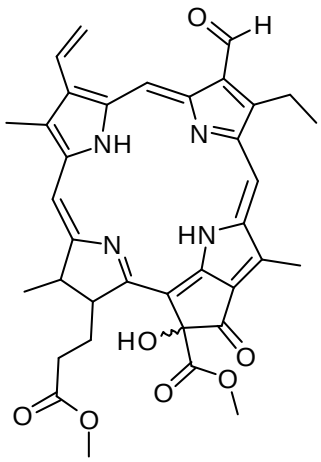

Figure 4.34: 13^2-hydroxypheophorbide-*b* methyl ester **(7)**

4.5.2.5 Identification of Cla-me-4-3

Cla-me-4-3 (5.2 mg) was categorized as chlorophyll-*b* type derivative based on its similar UV-Vis profile compared to Cla-me-4-2. Furthermore, the *m/z* analysis of the compound also gave a value of 637.30. However, the retention time of Cla-me-4-3 was

slightly longer than Cla-me-4-2 in RP-HPLC profile (R_t = 19.10 minutes). Figures 4.35 and 4.36 show the UV-Vis profile and LC-MS data of Cla-me-4-2.

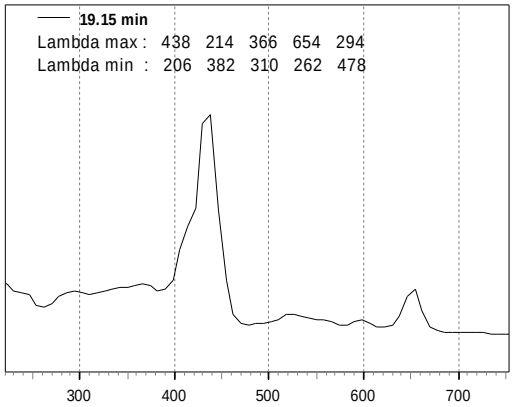

Figure 4.35: UV-Vis profile of Cla-me-4-3

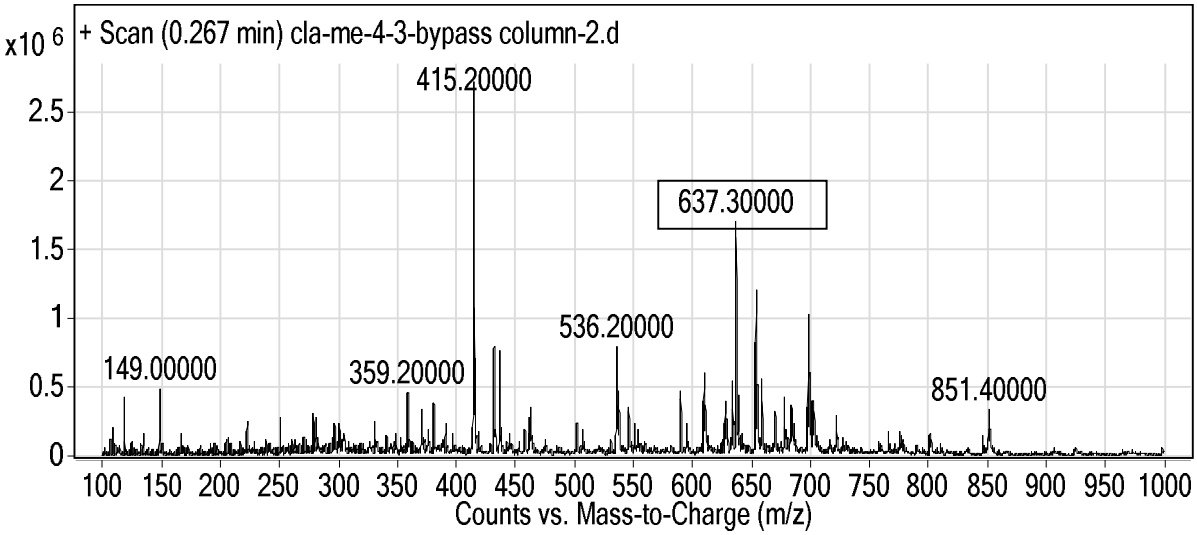

Figure 4.36: LC-MS data of Cla-me-4-3

The NMR data for Cla-me-4-3 (See Table 4.11) was similar to those of Cla-me-4-2 and the reported values of 13^2-Hydroxypheophorbide-*b* ethyl ester (Chee *et al.*, 2005), suggesting that Cla-me-4-2 to have the same structure as **(7)**, namely 13^2-hydroxypheophorbide-*b* methyl ester**.** They could be different in the stereoisomerism of hydroxyl group at C-13^2 due to the slight difference in the retention time observed in the HPLC profile (data not shown). However, determination of the stereochemistry of the compounds was not further attempted due to the lack of relevant 2D NMR data.

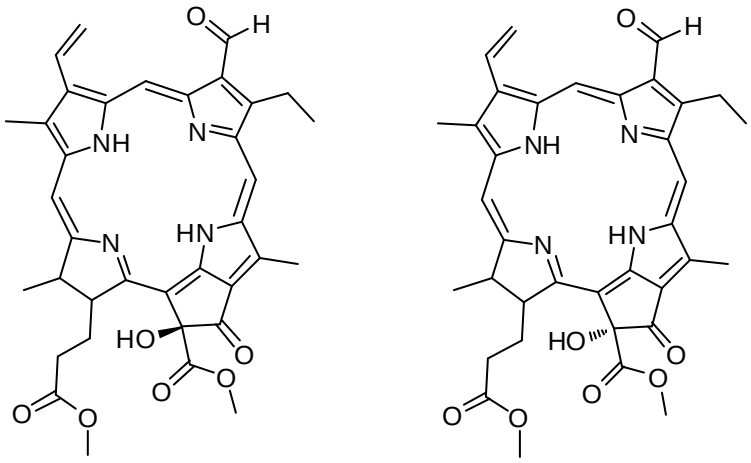

Figure 4.37: Possible Isomers of 13^2-hydroxypheophorbide-*b* methyl ester **(7)** and **(8)**

Table 4.11: ^{1}H NMR chemical shifts of Cla-me-4-3 in $CDCl_3$

Position of H	Chemical shift, δ(ppm) in $CDCl_3$, *J* in Hz		
	Cla-me-4-3	Cla-me-4-2	13^2 hydroxypheophorbide-*b* ethyl ester (Chee *et al.*, 2005)
17^3-OCH_2CH_3	-	-	1.19 (t, *J* = 7)
8^2-CH_3	1.89 (t, *J* = 8)	1.80 (t, *J* = 8)	1.86 (t, *J* = 8)
18-CH_3	1.63 (d)	1.62 (d, *J*=7)	1.73 (d, *J*=7)
17^2-CH_2	2.34-2.38 (m)	2.28 (t)	2.09 – 2.13 (m)
17^1-CH_2	2.57-2.60 (m)	2.31-2.41 (m)	2.56 – 2.63 (m)
2-CH_3	3.42 (s)	3.33 (s)	3.43 (s)
17^3-OCH_3	3.65 (s)	3.51 (s)	-
12-CH_3	3.68 (s)	3.59 (s)	3.66 (s)
8^1-CH_2	3.72 (m)	3.68 (m)	3.73 (q, *J* = 9)
13^2-CO_2CH_3	3.76 (s)	3.66 (s)	3.76 (s)
17-H	4.49 (br.d, *J* = 8)	4.59 (br.d, *J* = 8)	4.70 (br.d, *J* = 9)
18-H	4.16 (m)	4.40 (q, *J* = 7)	4.51 (q, *J* = 7)
13^2-OH	5.50(s)	5.25 (s)	5.58 (s)
3^2-CH_2	6.42 (d, *J* = 18)	6.33 (d, *J* = 18)	6.41 (d, *J* = 18)
	6.27 (d, J = 12)	6.18 (d, J = 12)	6.26 (d, J =12)
3^1-H	8.01 (dd, *J*=18,12)	7.92 (dd, *J*=18,12)	8.04 (dd, *J*=18,12)
20-H	8.63 (s)	8.52 (s)	8.64 (s)
5-H	10.53 (s)	10.71 (s)	10.47 (s)
10-H	9.82 (s)	9.71 (s)	9.74 (s)
7^1-CHO	11.24 (s)	11.15 (s)	11.17 (s)
NH	-1.58	-1.60	-1.62

4.5.2.6 Identification of Cla-me-4-5-4

Cla-me-4-5-4 (4.8 mg) was isolated and characterized as a chlorophyll-*b* derivative with Soret max of 430 nm and Q_y max of 654 nm based on the UV-Vis profile (See Figure 4.38). The mass value of Cla-me-4-5-4 was also acquired with the *m/z* value of 667.2913.

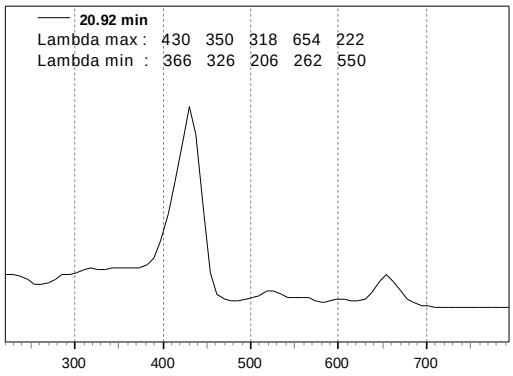

Figure 4.38: UV-Vis profile of Cla-me-4-5-4

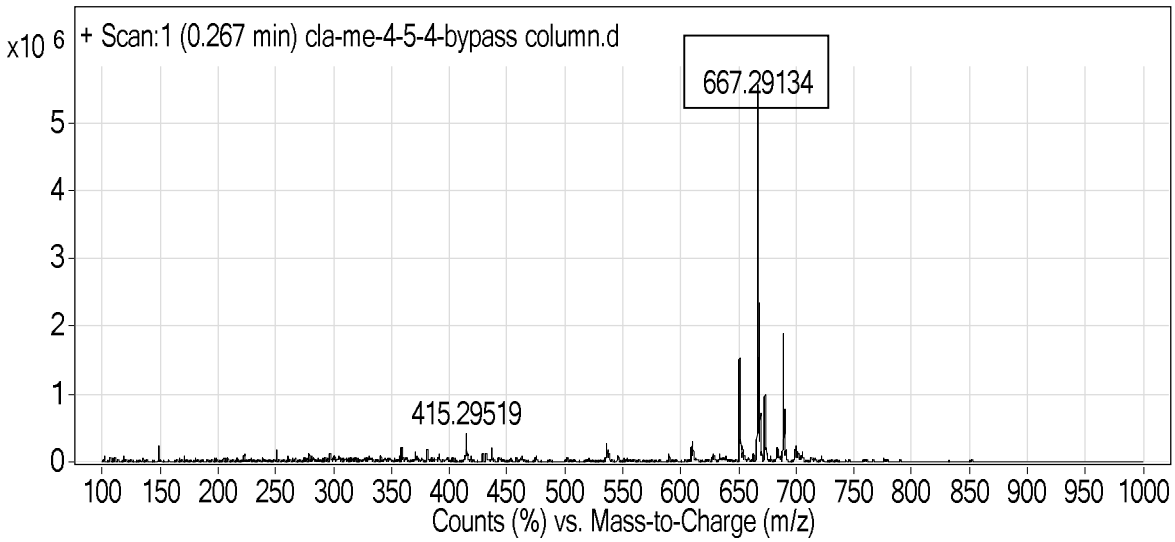

Figure 4.39: LC-MS data of Cla-me-4-5-4

Table 4.12: ^{1}H NMR chemical shifts of Cla-me-4-5-4 in $CDCl_3$

Position of H	Chemical shift, δ (ppm) in $CDCl_3$, *J* in Hz	
	Cla-me-4-5-4	5^1-methoxypurpurin-7-lactone methyl diester (Chee *et al.*, 2005)
17^3-OCH_2CH_3	-	1.10 (t, *J* = 7)
8^2-CH_3	1.87 (t)	1.75 (t)
18-CH_3	1.68 (d)	1.65 (d)
17^2-CH_2	not observed	2.44 – 2.50 (m)
17^1-CH_2	not observed	2.58 – 2.64 (m)
7-CH_3	-	3.32 (s)
2-CH_3	3.37 (s)	3.48 (s)
17^3-OCH_3	3.42 (s)	-
12-CH_3	3.51(s)	3.79 (s)
15^1-OCH_3	3.60 (s)	-
15^1-OH	-	5.60 (s)
15^1-CO_2CH_3	3.77 (s)	3.94 (s)
8^1-CH_2	3.71(br. d, *J* = 10)	3.82 (br. d, *J* = 9)
17-H	4.17 (m)	4.12 (br.d, *J* = 9)
18-H	4.50 (m)	4.50 (q, *J* = 7)
3^2-CH_2	6.41 (m)	6.38 (d, *J* = 18)
	6.27 (d)	6.23 (d, *J* = 12)
3^1-H_x	not observed	8.05 (dd, *J* = 18,12)
20-H	8.63 (s)	8.56 (s)
5-H	10.53 (s)	9.61 (s)
10-H	9.82 (s)	9.84 (s)
7-CHO	11.24 (s)	-
NH	-1.12	-1.02

The NMR data of Cla-me-4-5-4 (See Table 4.12) was compared with that of 15^1-hydroxypurpurin-7-lactone ethyl methyl diester (Chee *et al.*, 2005). The presence of a singlet peak at δ_H 11.24 that was assigned to an aldehyde group identified Cla-me-4-5-4 as a chlorophyll-*b* derivative. Furthermore, the presence of a methoxyl signal δ_H 3.60 and the absence of a hydroxyl signal suggested that the hydroxyl group was replaced by a methoxyl group at $C15^1$. The compound was proposed to be 7-formyl-15^1-methoxypurpurin-7-lactone methyl diester based on the NMR data (See Figure 4.40).

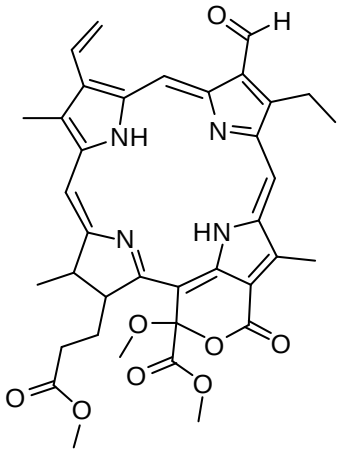

Figure 4.40: 7-formyl-15[1]-methoxy-7-lactone methyl diester **(9)**

4.6 Other semi-pure fractions

There were several semi-pure fractions which did not match any of the profiles of the known standards and other isolated compounds in the study. However, they were not further discussed in details due to inadequate NMR information for structure elucidation. Details of their UV-Vis profiles and *m/z* values are shown in Table 4.13.

Table 4.13: Characteristics of other semi-pure fractions from the seaweed extracts

Fractions	Source of Crude Extract	UV-Vis Profile (nm)	Mass value (*m/z*) $[M+H]^+$	Type of chlorophyll compound
Tur-10-4	Tur	406, 502, 670	653.3	*a*
Tur-17-6	Tur	406, - , 658	NIL	*a*
Tur-me-8-3	Tur-me	399, 655, 665	663.39	*a*
Cla-7-3	Cla	370, 434, 650	659.2	*b*

4.7 Photo-cytotoxicity of pure compounds

All the compounds described in the earlier sections showed variable photo-cytotoxicity in the MTT screening at 5 and 10 µg/mL (Figures 4.41 and 4.42). Seven compounds showed marked photo-cytotoxic killing at 5 µg/mL while Tur-19-1 and Tur-me-2 showed photo-cytotoxic killing only at 10 µg/mL.

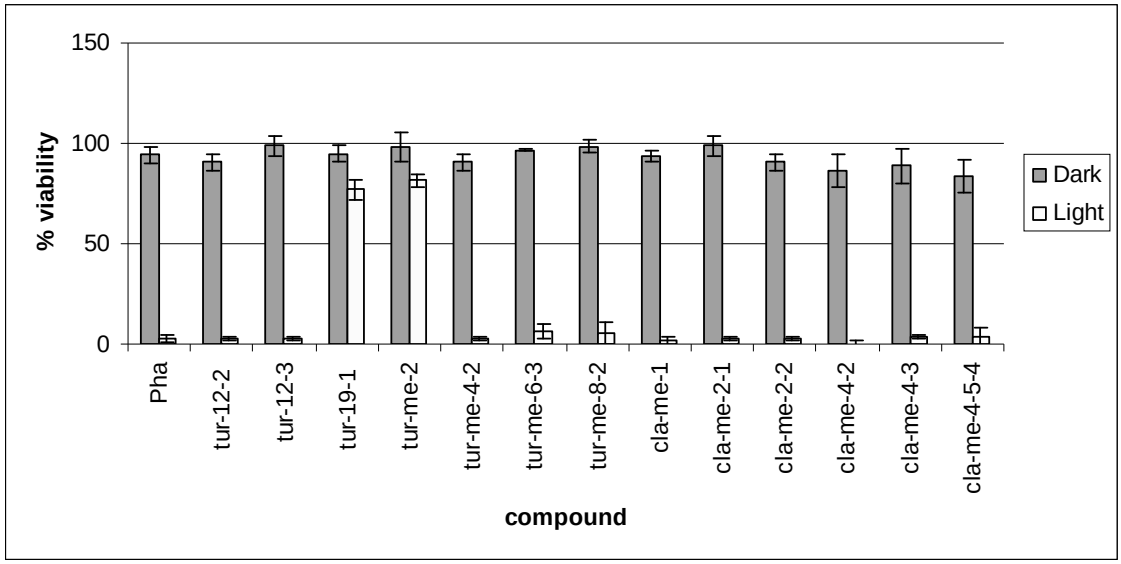

Figure 4.41: Viability of HL60 cells treated with the isolated compounds at 5 µg/mL

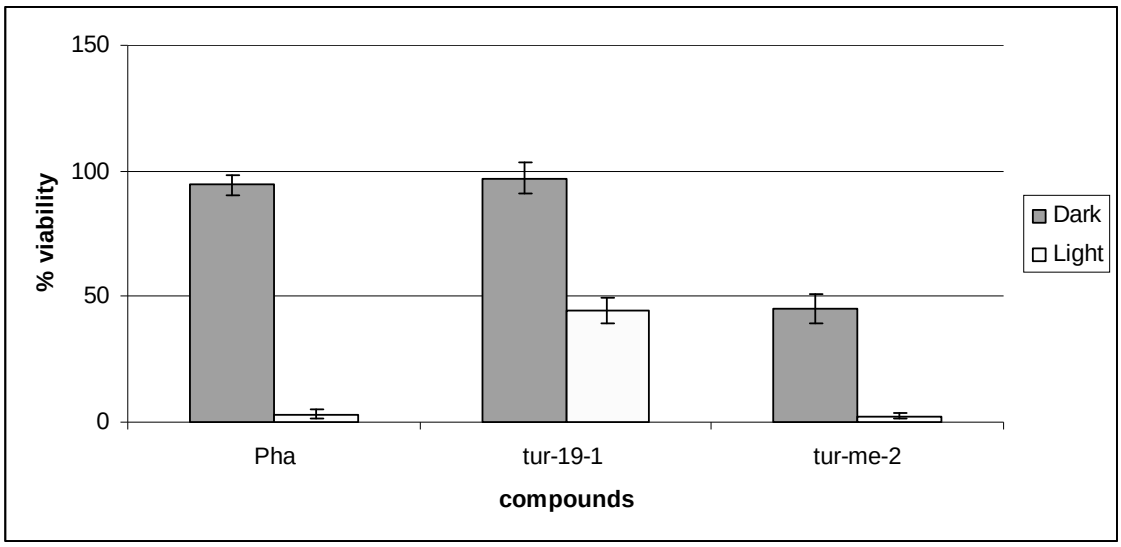

Figure 4.42: Viability of HL60 cells treated with Tur-unme-19-1 and Tur-me-2 at 10 µg/mL